

Monte Carlo Simulation of Electron Swarms in H₂

S. R. Hunter

School of Physical Sciences, Flinders University of South Australia,
Bedford Park, S.A. 5042.

Abstract

A Monte Carlo simulation of the motion of an electron swarm in molecular hydrogen has been studied in the range $E/N = 1.4-170$ Td. The simulation was performed for 400-600 electrons at several values of E/N for two different sets of inelastic collision cross sections at high E/N . Results were obtained for the longitudinal diffusion coefficient D_L , lateral diffusion coefficient D , swarm drift velocity W , average swarm energy $\langle \epsilon \rangle$ and ionization and excitation production coefficients, and these were compared with experimental data where available. It is found that the results differ significantly from the experimental values and this is attributed to the isotropic scattering model used in this work. However, the results lend support to the experimental technique used recently by Blevin *et al.* to determine these transport parameters, and in particular confirm their results that $D_L > D$ at high values of E/N .

1. Introduction

The motion of an electron swarm through a low pressure gas under the influence of a uniform electric field has been studied previously by two theoretical approaches, namely solution of the Boltzmann equation and Monte Carlo simulations of the processes occurring within the electron swarm. The Boltzmann equation can be solved numerically, as has been done by Engelhardt and Phelps (1963) and later by Crompton *et al.* (1969). Alternatively, numerous attempts have been made to obtain analytic solutions to the Boltzmann equation. These attempts and their validity have been outlined recently by Skullerud (1974) and Francey and Jones (1976). All these solutions fail at high values of E/N (E being the electric field strength and N the gas number density), where inelastic losses become the predominant energy loss mechanism, and similarly they also fail to describe the swarm development near material boundaries, where density and energy gradients can be large. These problems may be overcome by using Monte Carlo techniques to simulate the electron swarm development.

Several authors have used Monte Carlo techniques to study the rate of growth of ionization and the change in average energy with time in a number of gases (see e.g. Itoh and Musha 1960; Thomas and Thomas 1969; Folkard and Haydon 1970). Other authors have attempted to obtain a more complete description of the electron swarm transport parameters at lower values of E/N . Bell and Kostin (1968) obtained the drift velocity and energy distribution for helium and molecular hydrogen, and the lateral diffusion coefficient for nitrogen in the E/N range $0.006 \leq E/N \leq 0.6$ Td ($1 \text{ Td} = 10^{-17} \text{ V cm}^2$). Lucas (1972) is the only previous author to try to obtain diffusion coefficients at high E/N (30-140 Td) using a Monte-Carlo-Boltzmann

technique in helium. He obtained values for the lateral and longitudinal diffusion coefficients D and D_L respectively, the swarm drift velocity W , Townsend's first ionization coefficient α and the mean energy of the swarm $\langle \epsilon \rangle$. McIntosh (1974) determined corresponding transport parameters for helium at $E/N = 3.03$ Td. Lucas and Saelee (1975), using a similar technique to that of Lucas (1972), obtained a set of transport coefficients for a number of idealized collision models.

In general it is found that the transport parameters obtained by Monte Carlo simulations and by solution of the Boltzmann equation are in agreement only for restricted forms of the energy dependence of the collision cross section. There are no Monte Carlo simulations that have considered a molecular hydrogen Townsend discharge in the range $1 \leq E/N \leq 170$ Td, using recent theoretical and experimental cross sections for the inelastic processes and as accurate a collision model as possible. Thus a simulation of this nature should give information as to the validity of some of the cross sections obtained by theoretical methods, and to the application of the above theories to electron swarms in gases at high E/N . The other major reason for performing a Monte Carlo simulation in molecular hydrogen is that the results can be directly compared with the experimental work reported by Blevin *et al.* (1976*b*, 1976*c*). The longitudinal diffusion coefficients reported by these authors are the first to be obtained in the range $45 \leq E/N \leq 185$ Td, and it was therefore thought of value to develop a theoretical model with which to compare these results. The major assumption used by these authors is that the observed photon distribution is simply related to the actual electron distribution in the swarm (Blevin *et al.* 1976*a*). It is extremely important for this to be verified if their values for the drift velocity and longitudinal diffusion coefficient are to be accepted. It was thought that a Monte Carlo simulation would give supporting evidence that the photon distribution is indeed similar to the electron distribution, but displaced by a constant amount due to the energy variations across the swarm.

2. Monte Carlo Simulation Method

In the work reported here, the Monte Carlo method was used to simulate the motion of an electron swarm in molecular hydrogen within an E/N range $1.4 \leq E/N \leq 170$ Td. The gas molecules were assumed to be stationary and the simulation was carried out for $N = 3.56 \times 10^{16} \text{ cm}^{-3}$, corresponding to a temperature of 0°C and a pressure of 1.0 torr (~ 133 Pa). Both elastic and inelastic collisions were assumed to occur in the interaction of the electrons with the gas molecules. In an elastic collision an electron was assumed to lose a fraction $2m/M$ of its energy irrespective of scattering angle, where m is the electron mass and M the molecular mass. The simulation was performed for two different sets of inelastic cross sections in the range $56 \leq E/N \leq 170$ Td and for two sets of initial starting conditions in the range $1.4 \leq E/N \leq 11$ Td. This was done to show the effects of these parameters on the transport and production coefficients obtained. Isotropic scattering was assumed to occur in electron-molecule collisions. The reason for making this rather poor assumption in this initial study was that the angular distribution of scattered electrons from gas molecules is not very well known, particularly in the energy range from 0 to 10 eV where most of the electron-molecule collisions occur. Thus the results obtained do not give an accurate description of the collision processes occurring in the gas, but they should show approximately the variation

of the transport parameters with E/N and their sensitivity to changes in the various cross sections. These results will be helpful in the development of an anisotropic scattering model which is currently under investigation.

(a) *Collision model*

The total time between collisions is divided into from 1 to 100 intervals and a constant mean collision time appropriate to the electron energy is assumed for each interval. The number of intervals required is determined by the initial energy of the electron which is conveniently broken up into four ranges.

The first energy range is 15 eV and above. In this region, the total collision cross section used varies in such a way that the time T_c between collisions is almost independent of the energy of the electron. This approximation is valid because the difference in mean collision time corresponding to the energies at the beginning and end of a free path has been found to be 4% or less. This allows the actual collision time to be calculated from the expression $T_c = T_m \log(R1)$, where R1 is a random number equally probable between 0 and 1 and

$$T_m = (Q_T |V| N)^{-1} \quad (1)$$

is the mean collision time, which is inversely dependent on Q_T , the total collision cross section, $|V|$, the electron speed, and N , the gas number density.

The next energy range is $1.0 \leq \varepsilon \leq 15.0$ eV. The constant collision time model becomes unsatisfactory in this energy range as the difference in mean collision time before and after a mean free path has been traversed becomes large. It was decided to split the mean collision times into tenths and test for a collision after each step. The probability of a collision occurring in the time increment ΔT_c is given by

$$1.0 - \exp(-\Delta T_c/T_m),$$

where T_m is again the mean collision time, recalculated at the beginning of each tenth of a collision orbit. A series of random numbers is then called, the value of T_c is incremented by a tenth of T_m , and a new T_m is calculated at each step until a random number of value less than or equal to $1.0 - \exp(-0.1) = 0.0952$ is called, whereupon a collision is said to have taken place. The electron energy, position and velocity components are calculated at the end of each step. In this energy range, the difference in T_m at the beginning and end of each step is always less than 3%, and between 4 and 15 eV is less than 1%.

Below 1 eV, the above model again breaks down, and thus the time increment ΔT_c was made to be 1/100 of the mean collision time. The test for collision is carried out similarly to that for the 1.0–15.0 eV range, except that in this case the probability of a collision is $1.0 - \exp(-\Delta T_c/T_m) = 0.00995$. This approximation leads to a difference of less than 5% between collision times at the beginning and end of each step for the energy range 100 meV to 1.0 eV. The error rises to 15% at 45 meV. When an electron is found to have an energy of 45 meV or less at the end of a collision interval, the spatial and temporal coordinates are altered using Newton's equations of motion, such that the energy of the electron is increased to 50 meV. The V_z velocity component is then oriented against the electric field. The error in making this approximation is negligible for high values of E/N , but is expected to increase at the

lower end of the E/N range considered in this work. From the above description, it can be seen that the error in finding the collision time is always less than 5% in the energy range above 100 meV and rises to a maximum of 15% at 45 meV.

Allowance is made in the program for an electron to change into a different energy regime as it drifts between collisions, and the energy of the electron is found at a number of points in the program to ensure that it experiences the correct collision processes.

(b) Collision mechanics

Spherical coordinates are used in calculating the trajectory of the electron with the z axis oriented against the electric field E , that is, in the direction away from the cathode. In this coordinate system, the velocity components are given by the expressions

$$V_z = V \cos \theta, \quad V_x = V \sin \theta \cos \phi, \quad V_y = V \sin \theta \sin \phi.$$

The electrons are started initially from a point source with an emission energy ε_0 of 0.5 eV and randomly oriented such that $0 \leq \theta \leq \frac{1}{2}\pi$ and $0 \leq \phi \leq 2\pi$. At the beginning of each collision time increment T_c , the spatial and velocity components are found according to the expressions

$$\Delta z = V_z T_c + \frac{1}{2} E (e/m) T_c^2, \quad \Delta x = V_x T_c, \quad \Delta y = V_y T_c,$$

$$V_z = V_{z0} + E (e/m) T_c, \quad \varepsilon = (\frac{1}{2} m/e) (V_z^2 + V_x^2 + V_y^2)^{\frac{1}{2}}.$$

Electrons may be reflected back to the cathode whereupon they could be either absorbed or reflected. It was decided to use a reflection coefficient of 0.5 based on the results of Roberts and Burch (1964), who found the reflection coefficient for a gold electrode to be approximately constant over the energy range of interest.

After a collision has occurred, it is then determined whether the electron has collided elastically or experienced one of the several possible types of inelastic events, by calling a random number. These inelastic events are described in detail in the following subsection. When an elastic collision has occurred, the electron energy is decreased by the amount $2m/M$, while in an inelastic collision the electron is assumed to lose an amount of energy corresponding to the threshold for that particular process. If an ionizing event occurs, the energy remaining after subtracting the threshold energy is assumed to be shared randomly between the electrons, and the spatial, temporal and velocity coordinates of one electron are stored until the other electron has been tracked to the final printout time. The stored electron is then followed. No attempt has been made in the present work to include secondary ionization effects such as photon and positive ion bombardment of the cathode, which become important at high E/N for large transit times.

When a collision results in either dissociation, electronic excitation or ionization, the position and time of the event are stored for later analysis. The position and velocity components of the electron are stored after a number of finite time intervals, namely 0.05, 0.1, 0.2, 0.3, 0.4, 0.5 μ s. The total number of collisions and number of each type of inelastic event are also recorded. After the type of collision has been determined, the electron's velocity components are transformed into a coordinate system such that the velocity vector lies on the z axis. The angle ϕ is

randomly chosen from a uniform distribution on the interval $[0, 2\pi]$, while θ is calculated from the expression $\cos \theta = 2R - 1$, where R is a random number varying uniformly from 0 to 1.

(c) *Collision cross sections*

In the model described in this paper, a total collision cross section and several inelastic cross sections were used to simulate the type of collisions experienced by an electron on encountering a gas molecule. Owing to the uncertainties in trying to determine the dissociation and electronic excitation cross sections, two sets of these cross sections were used and their effect on the transport parameters was observed. The actual cross sections used in the simulation are described below.

Total Collision Cross Section

The total collision cross section used was that obtained by Golden *et al.* (1966) and covers the range from 200 meV to 15 eV. In the region 0–200 meV, the effective range formula determined by these authors was used. For the region 15–100 eV, the cross section obtained by Normand (1930) was used. This cross section is in reasonable agreement with that of Golden *et al.* in the region above 11 eV. The cross section is shown in Figs 1a and 1b.

Rotation Cross Sections

A number of theoretical and experimental determinations of the two main rotation state cross sections, namely the J_{0-2} and J_{1-3} transitions, have been made. The Linder and Schmidt (1971) J_{1-3} cross section, which agrees reasonably well with the cross section obtained by Gibson (1970), has been used in this work along with the J_{0-2} cross section of Crompton *et al.* (1969). In this initial study, no allowance has been made for the difference in the percentage population of the two rotation states in hydrogen which occur at 0°C. The threshold energies for these two states were assumed to be, for J_{0-2} , 45 meV and, for J_{1-3} , 75 meV.

Vibration Cross Sections

The cross section for vibrational excitation from the ground state to the first excited state obtained by Crompton *et al.* (1969) was used near threshold, and a smooth transition was made to the cross section of Ehrhardt and Linder (1968) at higher energies. For excitation to the second vibrational level, the cross section obtained by Ehrhardt and Linder was used. All higher levels were assumed not to contribute significantly to the energy loss. The threshold energies for the V_{0-1} and V_{0-2} states are 0.52 and 1.04 eV respectively. Fig. 1a shows the rotation and vibration cross sections used in the simulation.

Dissociation Cross Section

There are a number of higher energy states in molecular hydrogen, the lowest with a threshold of approximately 8.9 eV. For simplicity, these have been approximated to three cross sections in this study, namely a dissociation, electronic excitation and ionization cross section. To test whether these cross sections had a significant effect on the observed transport coefficients, two considerably different forms of the dissociation and electronic excitation cross sections were tried:

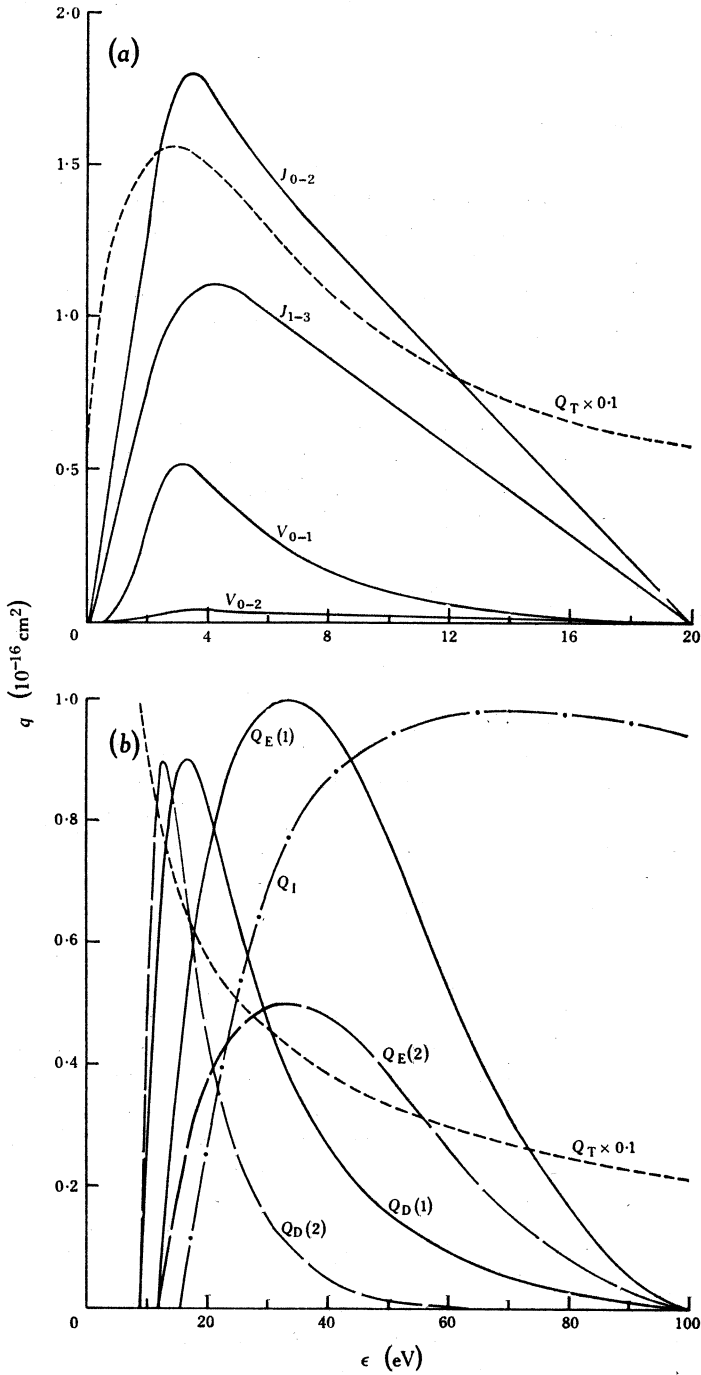


Fig. 1. Graphs of (a) the rotation and vibration cross sections J_{0-2} , J_{1-3} and V_{0-1} , V_{0-2} and (b) the two sets (1, 2) of the dissociation and excitation cross sections Q_D and Q_E and the ionization cross section Q_I used in the simulation. The adopted total cross section Q_T is shown in both figures.

(1) The initial dissociation cross section used was the one obtained by Corrigan (1965), which is approximately twice as large as that assumed by Engelhardt and Phelps (1963); the threshold energy for this process was assumed to be 8.9 eV.

(2) The second cross section to be tried had the same amplitude as that obtained by Corrigan (1965), but was compressed such that the area under the curve was about half that of the original cross section. The reason for changing the shape to this form was that it approximately agrees with the triplet excitation cross sections calculated by Prok *et al.* (1969) and experimentally measured by Trajmar *et al.* (1968).

Electronic Excitation Cross Section

As far as the author has been able to ascertain, there are no experimentally measured cross sections for singlet state electronic excitations reported in the literature. Hence it was decided to use the total electronic excitation cross section obtained by Engelhardt and Phelps (1963). This cross section is subject to large errors since it is very dependent on the form adopted for the dissociation cross section. A threshold energy of 12 eV was assumed for this process.

More recent calculations by Prok *et al.* (1969) and Heaps *et al.* (1975) indicate that the cross section of Engelhardt and Phelps (1963) is roughly twice as large as it should be for energies between 15 and 40 eV. Hence for the second set of cross sections, the excitation cross section was reduced by a factor of two to study the influence of this cross section on the transport parameters.

Ionization Cross Section

The total ionization cross section used in the simulation was that obtained by Cowling and Fletcher (1973). This process was assumed to have a threshold of 15.5 eV.

The higher inelastic cross sections used are shown in Fig. 1*b*.

(d) Discussion of collision model

A number of points must be raised about the collision model adopted and the random number generators used in the simulation. The reason for choosing a constant collision-time model rather than the more popular mean free path model is that there are computational difficulties in obtaining accurate radial displacements with the latter method. This is particularly true on tightly curved trajectories where the electron is travelling against the electric field with a low velocity. In the mean free path model, the electron will tend to persist travelling in a much shallower curve due to the fact that it is assumed to travel in straight lines between every tenth of a mean free path.

The collision model is more complex than might be expected for the following reasons. It was noticed early in this work that if only the tenth of a collision-time model was used for energies ≤ 1 eV, the energy distribution obtained was very highly peaked at low energies. There was also the problem that at these low energies it was possible to obtain unrealistically large collision times when equation (1) was used to calculate the mean collision time. Use of this equation assumes that the electron velocity does not change between each collision time interval T_c . This assumption gets progressively worse at lower electron velocities.

Owing to the problem of 'cycling' in pseudo random number sequences of relatively small cycle length, three independent number sequences were used in the code, with cycle lengths of greater than 10^9 numbers. Two of the sequences were used to determine the collision probability in each region, while the third was used wherever a random number was required for other purposes. With these sequences it is possible to follow many thousands of electrons before the chance of repetition becomes significant.

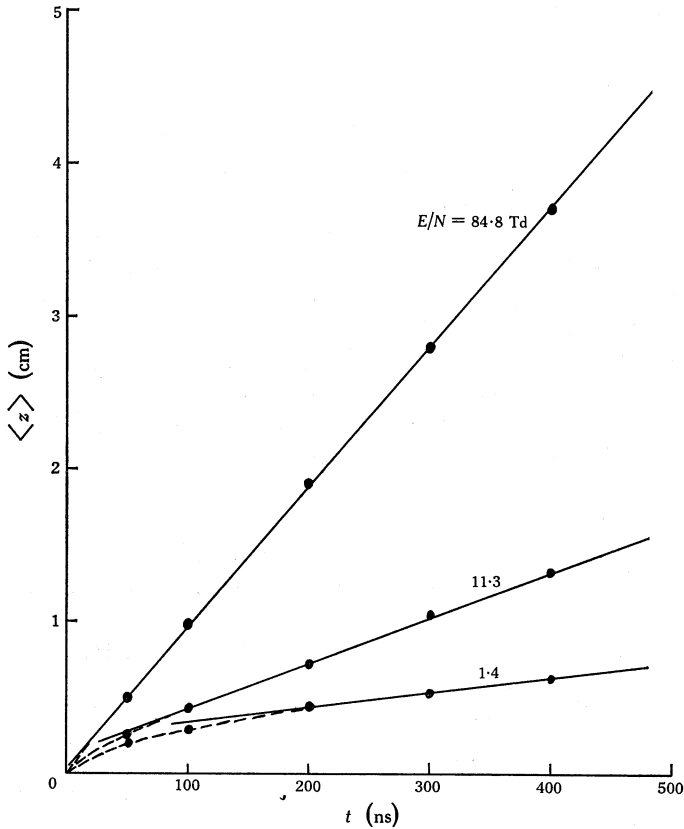


Fig. 2. Average z position as a function of the drift time t for three values of E/N .

3. Results

The simulation was run over the wide E/N range $1.4 \leq E/N \leq 170$ Td. For each E/N , between 400 and 600 electrons were followed and their positions, velocities and energies stored at six printout times. An analysis program was then run using the above results and the following parameters were determined at each printout time

$$\langle R^2 \rangle, \langle R \rangle^2, \langle z^2 \rangle - \langle z \rangle^2, \langle z \rangle, \langle \epsilon \rangle,$$

where $R = (x^2 + y^2)^{\frac{1}{2}}$ is the radial position of the electron. The values of D , D_L , W , D_L/μ and D/μ (μ being the mobility) were obtained from these parameters. As previously mentioned, the total number of each type of event was recorded, thus allowing the fractional power loss for each process to be found. The position and

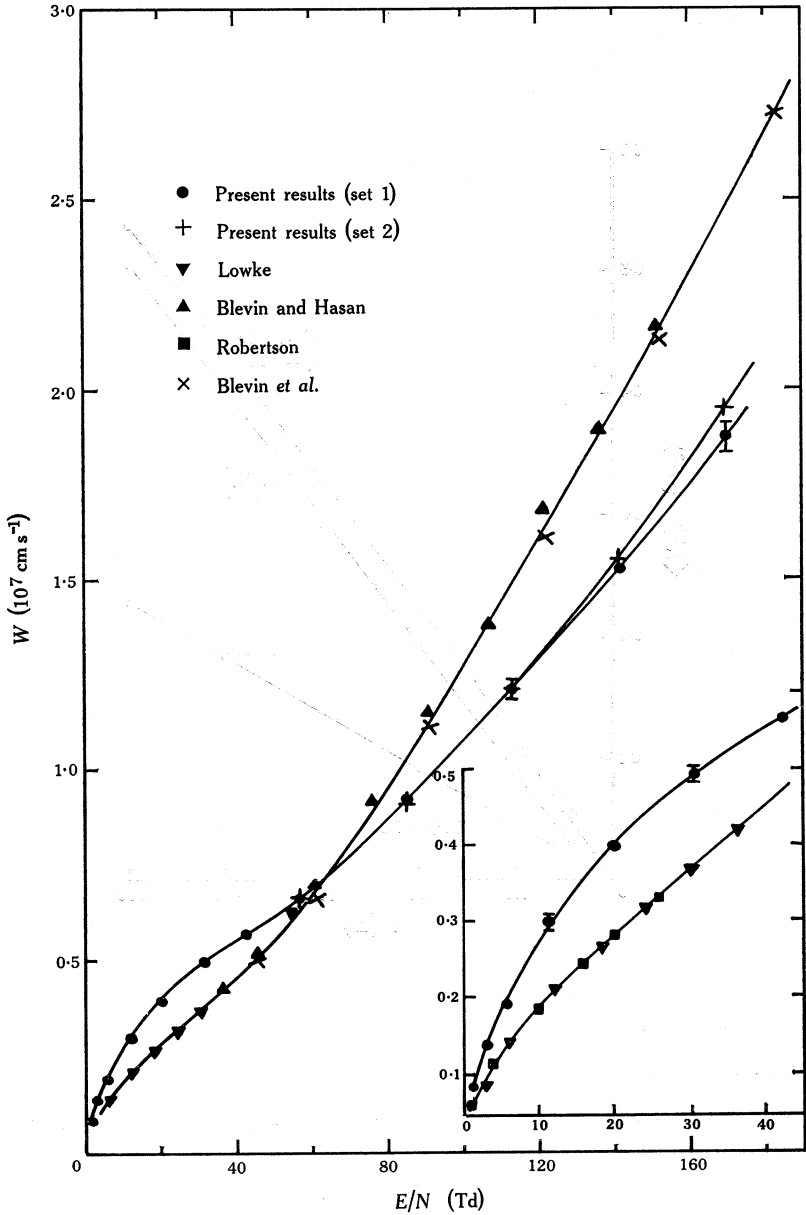


Fig. 3. Present results, obtained with two sets of inelastic cross sections, for the electron drift velocity W as a function of E/N compared with the experimental values of Lowke (1963), Blevin and Hasan (1967), Robertson (1971) and Blevin *et al.* (1976c). The inset gives an expanded graph at low E/N .

time of all dissociation, electronic excitation and ionization events were also recorded, allowing production coefficients, distributions and average positions of each event to be found. The simulation was performed for the two sets of cross sections described in Section 2c for the range $56 \leq E/N \leq 170$ Td and also for two different emission energies in the range $1.4 \leq E/N \leq 11$ Td to study the dependence of the transport parameters on the emission velocity.

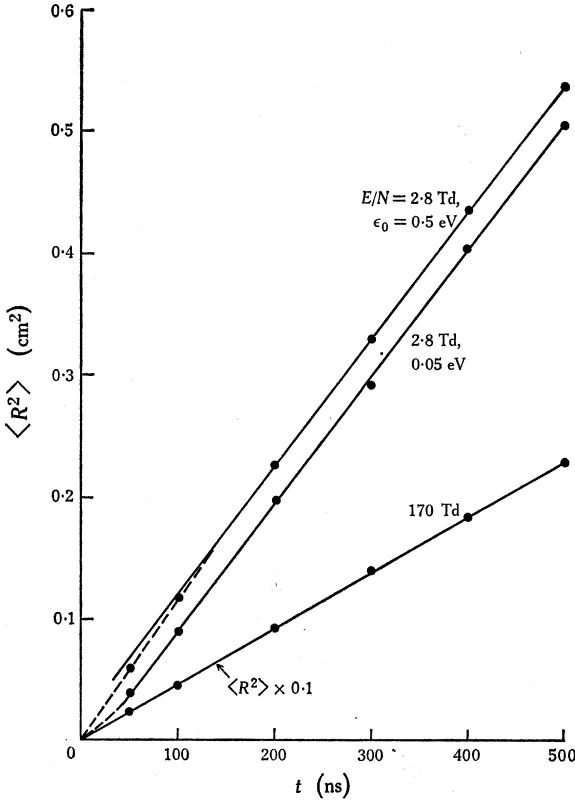


Fig. 4. Average of the radial position squared $\langle R^2 \rangle$ at several printout times for $E/N = 2.8$ and 170 Td and the two different emission energies ϵ_0 .

(a) Drift velocity

The average velocity of an electron swarm can be approximated by (Skullerud 1974)

$$\langle V \rangle = \langle z \rangle / t - \langle g_{01} \rangle / t,$$

where $\langle z \rangle$ is the average position of the swarm at time t and $\langle g_{01} \rangle = KD/W$, where K is a constant. Thus, for large t , $\langle g_{01} \rangle / t \rightarrow 0$ and the drift velocity $W \approx \langle z \rangle / t$. Alternatively, finding $d\langle z \rangle / dt$ when the swarm has attained equilibrium will give W . Three typical curves of $\langle z \rangle$ versus t are shown in Fig. 2. It can be seen that at low E/N the swarm takes a considerably longer time to reach equilibrium than at higher E/N . The values of W obtained from the slopes of these curves are given in Fig. 3, where they are compared with the results of Lowke (1963), Blevin and Hasan

(1967), Robertson (1971) and Blevin *et al.* (1976c). The graphs indicate that changing the cross sections has little effect on W except at large E/N . Similarly, reducing the emission energy from 0.5 to 0.05 eV has no observable effect on the equilibrium value of W , as is expected.

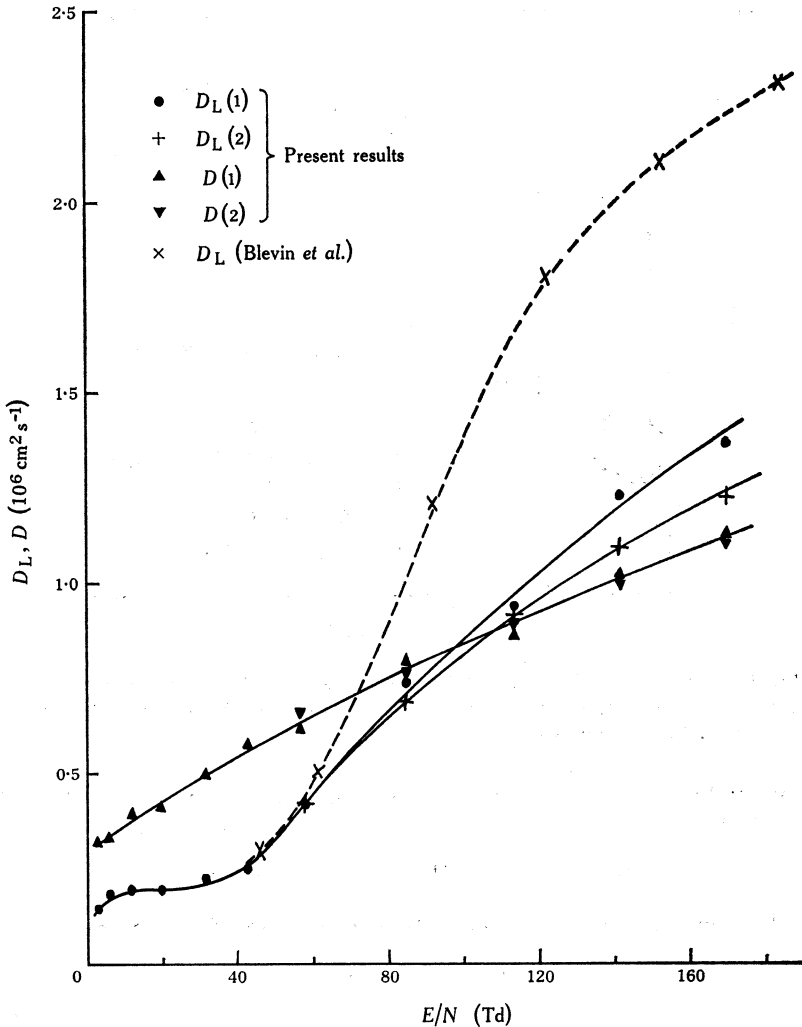


Fig. 5. Comparison of the two sets of present results for the longitudinal and lateral diffusion coefficients D_L and D as a function of E/N with the experimental values of Blevin *et al.* (1976c).

(b) Diffusion coefficients

The lateral diffusion coefficient D may be found from the relation (Skullerud 1974)

$$\langle R^2 \rangle = 4(Dt + \langle g_{20} \rangle),$$

where $\langle R^2 \rangle$ is the average of the square of the radial position and $\langle g_{20} \rangle$ is a constant that is dependent on the initial starting conditions. Consequently, when the difference

in $\langle R^2 \rangle$ is found after equilibrium has been obtained, D may be obtained as $D = \frac{1}{4} d\langle R^2 \rangle / dt$. It may also be found from the expression $D = \pi^{-1} d\langle R \rangle^2 / dt$, where the electron distribution is assumed to be gaussian in shape, which Skullerud has shown to be a valid approximation for large drift times. Both methods were used to find D and, in all cases, the differences between the results were less than 1%. Typical values of $\langle R \rangle^2$ are plotted in Fig. 4 for $E/N = 170$ and 2.8 Td.

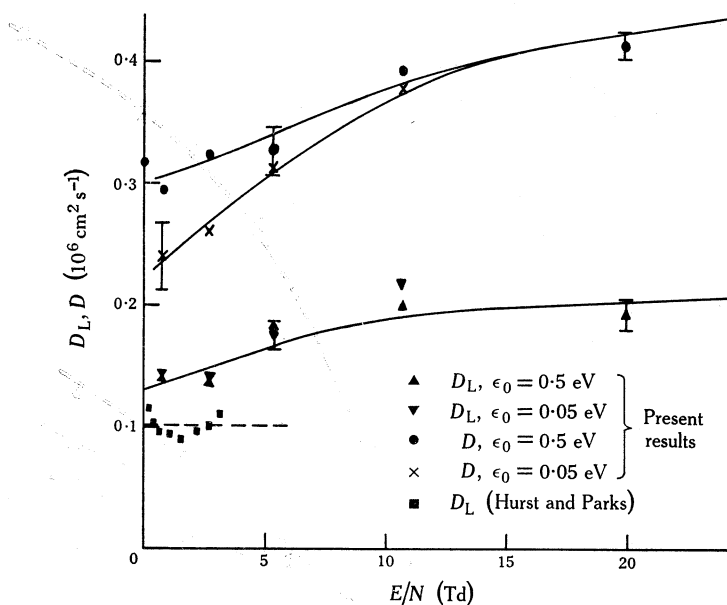


Fig. 6. Expanded graph of D_L and D at low values of E/N for the two emission energies ϵ_0 used. The experimental results of Hurst and Parks (1966) for D_L are included for comparison.

The longitudinal diffusion coefficient D_L may be found from the relation (Skullerud 1974)

$$\langle (z - \langle z \rangle)^2 \rangle = 2(D_L t + \langle g_{02} \rangle - \frac{1}{2} \langle g_{01}^2 \rangle).$$

By using the same arguments as above, D_L can be found from the expression

$$\langle z^2 \rangle - \langle z \rangle^2 = 2D_L t.$$

The values of D and D_L obtained from this analysis, for two different sets of cross sections, are summarized in Fig. 5, together with the experimental results of Blevin *et al.* (1976c). Changing the cross sections has had no effect on D that can be discerned from the graphs, as the points all lie within the stated uncertainty limits. On the other hand, D_L is more sensitive to these changes in cross sections, in that reducing the dissociation and excitation cross sections appreciably reduces D_L at higher E/N values.

Fig. 6 gives an expanded graph of the values of D and D_L at low E/N obtained with an emission energy of 0.5 eV and a fixed cathode, and also when the emission energy was reduced to 0.05 eV and the cathode removed. This was done in the hope that the time taken for the electrons to reach equilibrium would be considerably

reduced, and hence more accurate values of D and D_L could be obtained. The graphs show that D_L is relatively unaffected by a reduction in emission energy, while the apparent values of D are lower when the emission energy is reduced. This may be explained by examining the graphs in Fig. 4, which show that, for an emission energy of 0.5 eV, the swarm initially spreads much faster than at later times, giving a higher diffusion coefficient until it has lost enough energy to reach the average swarm

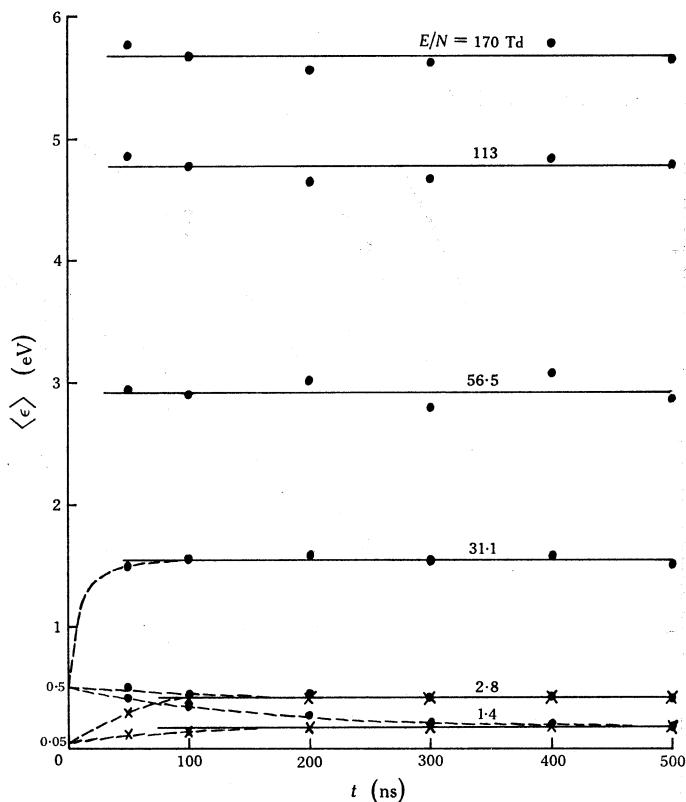


Fig. 7. Average swarm energy $\langle \epsilon \rangle$ as a function of the drift time t for six values of E/N and the two emission energies used.

energy. When started with an emission energy of 0.05 eV, the electron swarm has to gain energy to achieve equilibrium, giving a value of D that is too low. This apparent dependence of D upon emission energy results from equilibrium not being achieved in the drift times used, and it is expected that the true value of D lies between the values shown in Fig. 6. The value of D_L is unaffected since it is obtained by the difference between $\langle z \rangle^2$ and $\langle z^2 \rangle$ and any errors in $\langle z \rangle^2$ would be of the same order in $\langle z^2 \rangle$ (as also occurs for $\langle R \rangle^2$ and $\langle R^2 \rangle$). Hence the value of D_L obtained should be reasonably accurate.

It may be noticed from Figs 7 and 8 that the average swarm energy at approximately $E/N = 8$ Td is 0.5 eV, and it is in this region that the two diffusion coefficients measurements converge to within the statistical errors quoted. It appears then that, by starting the electron with an energy approximately the same as its final average equilibrium energy, the swarm will thereby achieve an equilibrium distribution

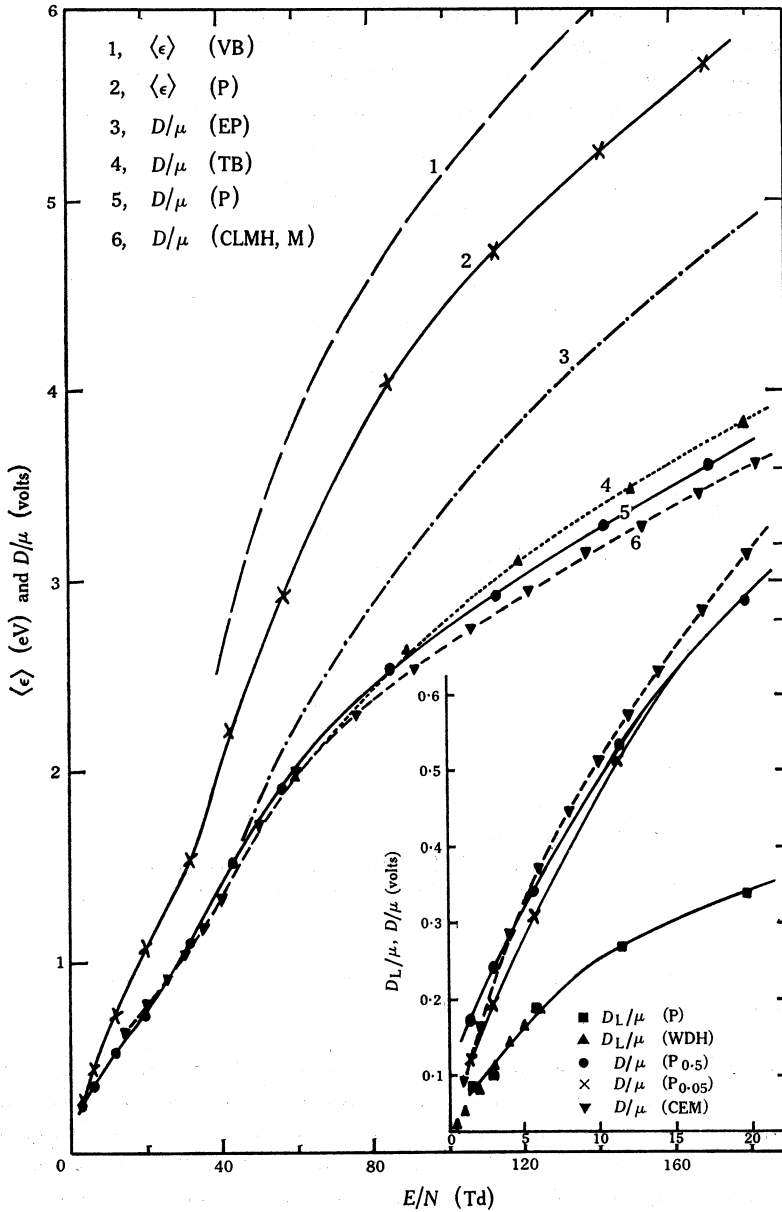


Fig. 8. Comparison of the present results (P) for D_L/μ , D/μ and $\langle \epsilon \rangle$ as a function of E/N with the previous values of (VB) Varnerin and Brown (1950), (EP) Engelhardt and Phelps (1963), (TB) Townsend and Bailey (1921), (CLMH) Crompton *et al.* (1965), (M) McIntosh (1965), (WDH) Wagner *et al.* (1967) and (CEM) Crompton *et al.* (1968). The present results for both emission energies used ($P_{0.5}$ and $P_{0.05}$) are included in the inset, which is an expanded graph at low E/N .

at earlier drift times and hence a more accurate value of D may be obtained. This is in agreement with the work of Skullerud (1974), in that if the electrons are started with the equilibrium energy distribution then their time-dependent constants go to zero. This may also be seen from Fig. 7, which shows the time taken for the swarm to achieve an equilibrium energy distribution for several values of E/N and for starting energies of 0.5 and 0.05 eV. At high E/N the swarm rapidly attains an equilibrium distribution, but requires a longer time at lower values of E/N . Thus the values of D at high E/N can be assumed to be correct for this model while those at low E/N with a starting energy well above the final average energy will have a larger D/μ , and hence D , than the final equilibrium value.

(c) D/μ values and average energy

Fig. 8 shows the variation of D/μ , D_L/μ and $\langle \varepsilon \rangle$ as a function of E/N , as obtained by the Monte Carlo simulation, compared with previous results. It can be seen from the figure that the values of D/μ obtained are in fair agreement with experiment, as are the values of D_L/μ when compared with those of Wagner *et al.* (1967) at low E/N . The values of $\langle \varepsilon \rangle$ obtained by Varnerin and Brown (1950) using a microwave technique are larger than the present results. This is also the case for the values of D/μ calculated by Engelhardt and Phelps (1963). Preliminary work using an anisotropic scattering model has given results for D/μ which similarly are in better agreement with those of McIntosh (1965) and of Townsend and Bailey (1921) than those of Engelhardt and Phelps. This has important consequences for the cross sections obtained by Engelhardt and Phelps, who assumed that the values of D/μ obtained by Townsend and Bailey were too low. This gave them a total momentum transfer cross section Q_m which appeared to be too large, but they decided to leave the computed values as they were, owing to lack of more recent data at high E/N . The results of Crompton *et al.* (1965) and McIntosh (1965) lend support to the values obtained by Townsend and Bailey, indicating that Engelhardt and Phelps were wrong in their assumption. The conclusion that their values of Q_m are too large at high energies is consistent with experimental measurements of the total scattering cross section and angular scattering data. Since the excitation and dissociation cross sections obtained by them are dependent on the value of the momentum transfer cross section, the modified cross sections were chosen here on the basis of the results of Trajmar *et al.* (1968) and Prok *et al.* (1969).

(d) Production coefficients

The Monte Carlo simulation can also be used to determine the production coefficients for the various inelastic processes that occur within the swarm. The values obtained for Townsend's primary ionization coefficient α/p , are shown in Fig. 9 for the two different sets of cross sections, compared with the values obtained by Rose (1956) and Chanin and Rork (1963). Figs 10a and 10b show the electronic excitation and dissociation coefficients ε/p and χ/p respectively compared with those obtained by Corrigan and Von Engel (1958) and Poole (1937). The values of α/p are too low for both sets of cross sections used, but considerably better when Q_D and Q_E have been modified. Similarly, ε/p and χ/p are well below the values obtained by Corrigan and Von Engel. Part of the explanation for the reduced coefficients can be seen by reference to Fig. 11 and to Corrigan and Von Engel's paper. They analysed the energy losses due to each mechanism at $E/N = 121$ and 303 Td. At 121 Td they

assumed that the rotational losses were negligible and the vibrational contribution was 5%. Fig. 11 indicates that the total rotational and vibrational losses are at least 23% of the total loss. Hence it is impossible to achieve the production coefficients presented in their paper. A number of difficulties can be seen in their technique for obtaining these coefficients, particularly in the calibration of the detection system to measure the photon flux from the discharge and also the assumption that the reduction in pressure in the determination of the rate of dissociation is entirely due to absorption of atomic hydrogen by the molybdenum trioxide (Corrigan 1965). These two problems may give coefficients which are too high.

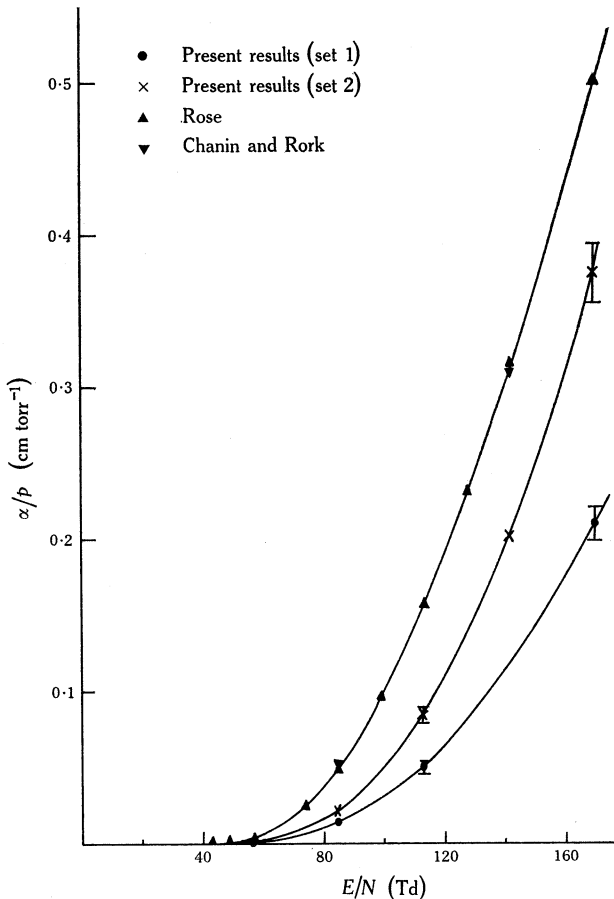


Fig. 9. Comparison of the present results for Townsend's first ionization coefficient α/p , obtained with the two sets of inelastic cross sections, with the experimental values of Rose (1956) and Chanin and Rork (1963).

The reason for the present low ionization coefficient is less obvious. To force agreement between the experimental and Monte Carlo results, the dissociation and excitation cross sections would have to be further significantly reduced. This would appear to give cross sections for dissociation and excitation which are too small when compared with previous work by Corrigan (1965) and Trajmar *et al.* (1968). Similarly, it is difficult to justify any reduction in the vibration or rotation cross

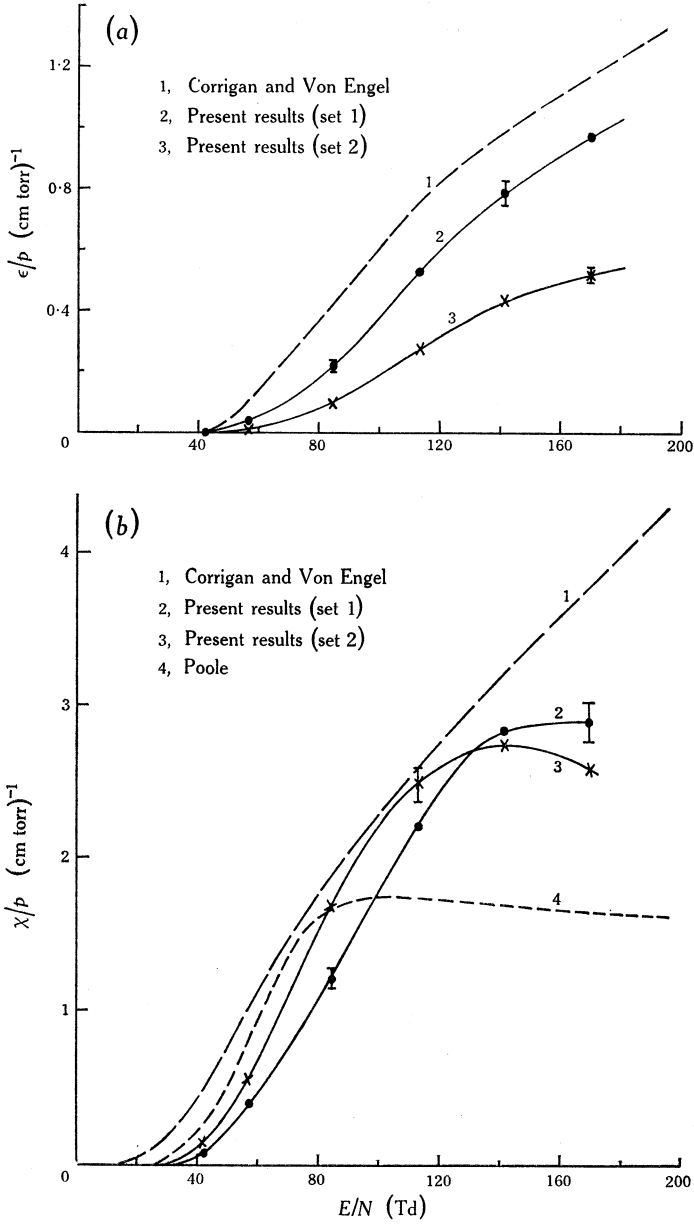


Fig. 10. Comparison of the present results for (a) the electronic excitation coefficient ϵ/p and (b) the dissociation coefficient χ/p with the experimental values of Corrigan and Von Engel (1958) and Poole (1937).

sections which have been determined experimentally at high energies, while at lower energies near threshold the agreement with experimentally derived transport coefficients is such that they can only be in error by a few per cent. Drastic reductions in these cross sections would be required to raise the ionization coefficient significantly at high E/N values. It would appear that the discrepancy in α/p could be a consequence of the isotropic scattering model used in the present work, resulting in a momentum transfer cross section which is too large at high energies.

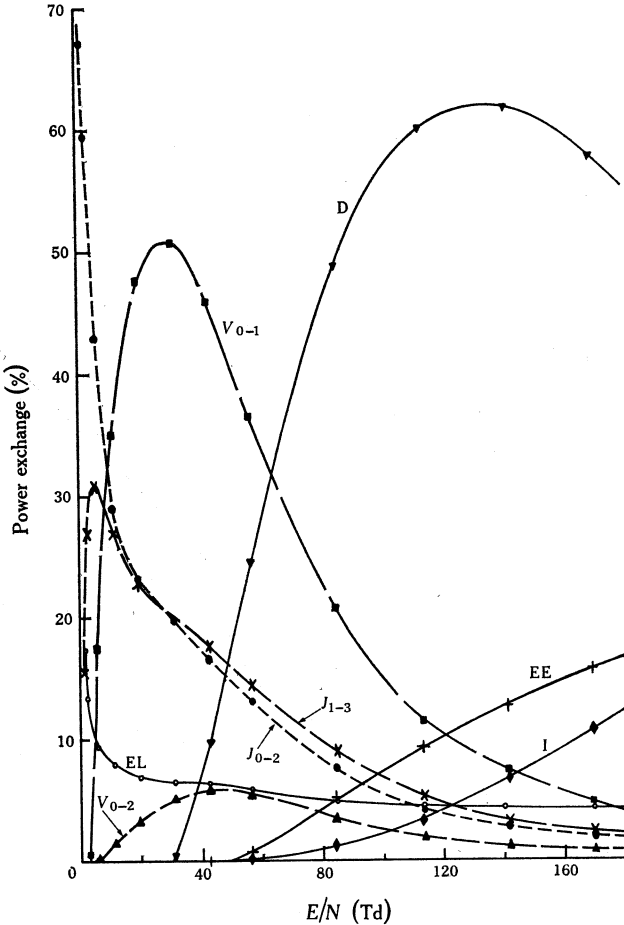


Fig. 11. Percentage power lost by an electron in collision with hydrogen molecules. The curves show the elastic (EL) and inelastic losses due to dissociation (D), electronic excitation (EE), ionization (I) and rotational and vibrational excitation (dashed curves).

(e) Relationship between photon production and electron position

One of the major reasons for initiating this work was to try to show that the assumptions made in the experimental work of Blevin *et al.* (1976a, 1976b, 1976c) are valid. They assumed that the average position of photon production in the swarm is slightly in front of the average position of the electron distribution, but remains the same distance in front once the swarm has reached equilibrium. This

assumption was found to be true when a model using a simple form for the energy variation across a swarm was calculated (Blevin *et al.* 1976a). To find the average positions at which photons are produced using the Monte Carlo model, it is too time consuming to look at photons in a very small range of time as few photons are produced during the transit time. To try to improve the statistics at, for example, a printout time of 300 ns all photons produced between 250 and 350 ns were used. The difference in time between production and printout was found, and the position of production was incremented or subtracted by the product of its time difference and the drift velocity of the swarm as a whole. Thus, if the photons were being produced progressively towards the front of the swarm, the difference in average position of the electrons and photons would not remain constant. Fig. 12 shows two typical sets of graphs obtained for photon production rates at $E/N = 85$ and 170 Td. The difference between average photon and electron positions remains constant for a given E/N , but decreases as E/N increases. Additionally it may be noticed that the position of ionization found by the same method also gives a constant difference, indicating that the drift velocity of the photon and ionizing events is the same as that of the electron swarm as a whole, once the swarm has reached equilibrium. These results indicate that the values of drift velocity obtained by Blevin *et al.* using this technique are not likely to be in serious error.

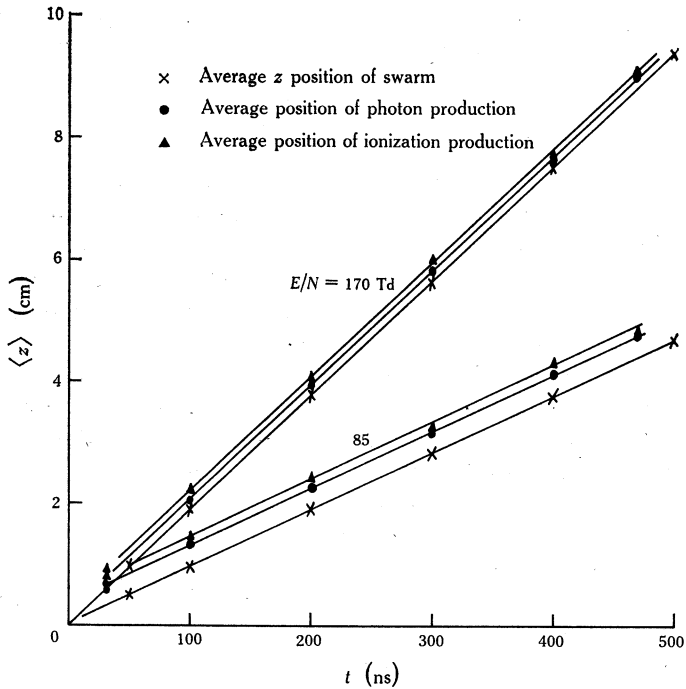


Fig. 12. Average swarm position and photon production and ionization production positions for several printout times at two values of E/N .

(f) Errors

It was found that varying numbers of electrons per swarm were required to specify a particular transport coefficient to a given degree of accuracy. To measure W to within 2%, approximately 200 electrons were required, as variation in W between

groups of this size always gave a value that agreed with other groups of similar size to within $\pm 2\%$. Hence the error bars of $\pm 2\%$ shown in Fig. 3 are a conservative estimate for the 400–600 electrons used in these calculations at each value of E/N , and any reason for the difference between the curve obtained by the Monte Carlo method and that obtained experimentally must be found elsewhere. At higher values of E/N approximately 400 electrons were required to obtain values of D with a scatter of 2% or less between groups. For a swarm of this size, the difference in D obtained by the two previously mentioned methods was always less than 1%. At lower values of E/N , D became more uncertain owing to the longer time required for the swarm to reach equilibrium. The printout times in this model were fixed because of the excessive computing time required for longer drift times. Thus, below $E/N \approx 10$ Td the error becomes significantly larger, to an estimated 10% at $E/N \approx 1.4$ Td. Since D_L is obtained by the difference between $\langle z \rangle^2$ and $\langle z^2 \rangle$, the errors in each quantity must add to give a value of approximately 5% for this parameter. The value of D_L appears to be relatively unaffected when the emission energy is changed, for the reason mentioned in Section 3*b*, and hence the error in D_L is quoted at $\pm 5\%$ over the entire range of E/N . The scatter in $\langle \varepsilon \rangle$ was around $\pm 5\%$ when the swarm appeared to have reached equilibrium. A similar error is placed on the production coefficients. The error in obtaining the ‘drift velocity’ of the photons in Fig. 12 is estimated to be $\pm 2\%$ from the scatter of the points. Thus it is assumed that the drift velocity of the observed photons is the same as that of the swarm as a whole to within $\pm 2\%$ over the range $56 \leq E/N \leq 170$ Td.

4. Conclusions

From an examination of the preceding results, it can be seen that there are wide discrepancies between the previously published transport parameters and those reported here, and that these discrepancies lie well outside the range of the statistical errors discussed above. There are two possible reasons for these discrepancies, only one of which has been studied in this work. Firstly, the inelastic cross sections which have been used may be incorrect, giving erroneous energy distributions which will affect the derived transport coefficients and, secondly, the assumption that the electrons are scattered isotropically in collisions with the gas molecules is incorrect. The first possibility has been studied in the simulation by using two different photon and dissociation cross sections. It has been seen that, for the upper range of E/N considered, changing the cross sections does affect the drift velocity and diffusion coefficients but not to a large extent, certainly not enough to give agreement between the experimental and Monte Carlo results. It must be noted that since no allowance was made for the variation in the percentage population of the two rotation states, the rotation cross sections used are thus too large. This problem has only a minor effect on the derived transport parameters for higher E/N values, as has been found in the initial anisotropic scattering studies.

Thus, as expected, anisotropic scattering must play an important part in the determination of the swarm parameters. The recent angular scattering data of Trajmar *et al.* (1970), Lloyd *et al.* (1974) and Teubner *et al.* (1974) indicate that above 10 eV the electrons become highly forward scattered. Ehrhardt *et al.* (1968) and Linder and Schmidt (1971) have shown that below 2.0 eV the electrons are highly backward scattered when colliding with hydrogen molecules, while in the range

2.0–5.0 eV most electrons are scattered either in the forward or reverse direction with few being scattered at 90° with respect to the incident direction. This is supported by Crompton *et al.* (1969) who have deduced that below 3.5 eV the momentum transfer cross section is higher than the total scattering cross section, while above 3.5 eV and up to the limit considered in their work the momentum transfer cross section is lower. Qualitatively then, it can be seen that for high average energies the electrons will be scattered predominantly in the forward direction, raising the drift velocity and diffusion coefficients, while at lower E/N , where the average energy is much lower, the scattering will be in the reverse direction giving smaller values for the transport coefficients. It should be noted that, at relatively high incident energies, the elastic momentum transfer cross section should be very much lower than the total scattering cross section, but the cross section used by Engelhardt and Phelps (1963) is very nearly the same as the total scattering cross section, indicating that their cross sections are too high as noted in Section 3c.

Even allowing for these large discrepancies, a number of important conclusions can be drawn from this work. Firstly, it appears that it is valid to assume that the average drift velocity of the electron swarm is the same as that of the photons to within the stated error, verifying the drift velocity measurements of Blevin *et al.* (1976*b*, 1976*c*). It should be noted that the drift velocity quoted here is for the whole swarm and not only the initial electrons, and is thus directly related to the experimental results of Blevin *et al.* No attempt has been made to quantitatively see if the photon distribution is the same as the electron distribution from the simulation results, as many more electrons are required to be followed before the statistics become reasonable. But the results obtained from the simulation do tend to suggest that the shapes of the electron and photon distributions are the same, allowing the diffusion coefficients to be obtained by the method used by Blevin *et al.*

The second major point to arise from this work is the variation in the ratio of the longitudinal diffusion coefficient to the lateral diffusion coefficient as a function of E/N . It can be seen that, at low E/N , the ratio is approximately one half, agreeing with the theoretical work of Skullerud (1974), when elastic scattering and low loss inelastic processes are the predominant energy loss mechanisms. At higher values of E/N , D_L increases faster than D until they cross at $E/N = 95$ Td. The only other theoretical work to show this tendency is that reported by Lucas (1970), who obtained the ratio $D_L/D = 1$ at $E/N = 85$ Td. This is also in approximate agreement with the experimental results of Blevin *et al.* (1976*c*) which show that $D_L = D$ at approximately $E/N = 80$ Td.

Work is now in progress to allow for the anisotropy in the scattering of electrons from molecular hydrogen as reported above, to see if more realistic values of the diffusion coefficients and drift velocity can be obtained. Variations in the average energy across the swarm with time and the relationship between the electron distribution and the observed photon distribution will be studied in much greater detail to see if the diffusion coefficients obtained from both distributions are the same. Early work on the anisotropic scattering model does indicate that the transport parameters are very considerably affected by the angular distribution of the scattered electrons. The work described here has demonstrated the degree of sensitivity obtained in the calculated values of the transport parameters to changes in the various cross sections. This will greatly assist in the choice of cross sections to be used in fitting the anisotropic scattering calculations to experimental data.

Acknowledgments

The author would like to thank Professor H. A. Blevin for his support and assistance. A Commonwealth Postgraduate Research Scholarship was held during this study.

References

- Bell, M. J., and Kostin, M. D. (1968). *Phys. Rev.* **169**, 150.
- Blevin, H. A., Fletcher, J., and Hunter, S. R. (1976c). *J. Phys. D* **9**, 1671.
- Blevin, H. A., Fletcher, J., Hunter, S. R., and Marzec, L. M. (1976b). *J. Phys. D* **9**, 471.
- Blevin, H. A., Fletcher, J., and Marzec, L. M. (1976a). *J. Phys. D* **9**, 465.
- Blevin, H. A., and Hasan, M. Z. (1967). *Aust. J. Phys.* **20**, 735.
- Chanin, L. M., and Rork, G. D. (1963). *Phys. Rev.* **132**, 2547.
- Corrigan, S. J. B. (1965). *J. Chem. Phys.* **43**, 4381.
- Corrigan, S. J. B., and Von Engel, A. (1958). *Proc. R. Soc. London A* **245**, 335.
- Cowling, I. R., and Fletcher, J. (1973). *J. Phys. B* **6**, 665.
- Crompton, R. W., Elford, M. T., and McIntosh, A. I. (1968). *Aust. J. Phys.* **21**, 43.
- Crompton, R. W., Gibson, D. K., and McIntosh, A. I. (1969). *Aust. J. Phys.* **22**, 715.
- Crompton, R. W., Liley, B. S., McIntosh, A. I., and Hurst, C. A. (1965). Proc. 7th Int. Conf. on Phenomena in Ionized Gases, Beograd, Vol. 1, p. 86 (Gradevinska Knjiga: Beograd).
- Ehrhardt, H., Langhans, L., Linder, F., and Taylor, H. S. (1968). *Phys. Rev.* **173**, 222.
- Ehrhardt, H., and Linder, F. (1968). *Phys. Rev. Lett.* **21**, 419.
- Engelhardt, A. G., and Phelps, A. V. (1963). *Phys. Rev.* **131**, 2115.
- Folkard, M. A., and Haydon, S. C. (1970). *Aust. J. Phys.* **23**, 847.
- Francey, J. L. A., and Jones, D. A. (1976). *J. Phys. D* **9**, 457.
- Gibson, D. K. (1970). *Aust. J. Phys.* **23**, 683.
- Golden, D. E., Bandel, H. W., and Salerno, J. A. (1966). *Phys. Rev.* **146**, 40.
- Heaps, M. G., Furman, D. R., and Green, A. E. S. (1975). *J. Appl. Phys.* **46**, 1798.
- Hurst, G. S., and Parks, J. E. (1966). *J. Chem. Phys.* **45**, 282.
- Itoh, T., and Musha, T. (1960). *J. Phys. Soc. Jpn* **15**, 1675.
- Linder, F., and Schmidt, H. (1971). *Z. Naturforsch* **26a**, 1603.
- Lloyd, C. R., Teubner, P. J. O., Weigold, E., and Lewis, B. R. (1974). *Phys. Rev. A* **10**, 175.
- Lowke, J. J. (1963). *Aust. J. Phys.* **16**, 115.
- Lucas, J. (1970). *Int. J. Electron.* **29**, 465.
- Lucas, J. (1972). *Int. J. Electron.* **32**, 393.
- Lucas, J., and Saelee, H. T. (1975). *J. Phys. D* **8**, 640.
- McIntosh, A. I. (1965). Q. Rep. Ion Diffusion Unit, Aust. Nat. Univ., Canberra, No. 20, p. 1.
- McIntosh, A. I. (1974). *Aust. J. Phys.* **27**, 59.
- Normand, C. E. (1930). *Phys. Rev.* **35**, 1217.
- Poole, H. G. (1937). *Proc. R. Soc. London A* **163**, 424.
- Prok, G. M., Monnin, C. F., and Hettel, H. J. (1969). *J. Quant. Spectrosc. Radiat. Transfer* **9**, 361.
- Roberts, T. D., and Burch, D. S. (1964). *Rev. Scient. Instrum.* **35**, 1067.
- Robertson, A. G. (1971). *Aust. J. Phys.* **24**, 445.
- Rose, D. J. (1956). *Phys. Rev.* **104**, 273.
- Skullerud, H. R. (1974). *Aust. J. Phys.* **27**, 195.
- Teubner, P. J. O., Lloyd, C. R., and Weigold, E. (1974). *Phys. Rev. A* **9**, 2552.
- Thomas, R. W. L., and Thomas, W. R. L. (1969). *J. Phys. B* **2**, 562.
- Townsend, J. S., and Bailey, V. A. (1921). *Philos. Mag.* **42**, 873.
- Trajmar, S., Cartwright, D. L., Rice, J. K., Brinkmann, R. T., and Kuppermann, A. (1968). *J. Chem. Phys.* **49**, 5464.
- Trajmar, S., Truhlar, D. G., Rice, J. K., and Kuppermann, A. (1970). *J. Chem. Phys.* **52**, 4516.
- Varnerin, L. J., and Brown, S. C. (1950). *Phys. Rev.* **79**, 946.
- Wagner, E. B., Davis, F. J., and Hurst, G. S. (1967). *J. Chem. Phys.* **47**, 3138.